BMC Plant Biology

RESEARCH

Open Access

Transcriptomic insights into the synergistic effects of darkness and mechanical stimulation on peanut pod development

Lu Huang[1†], Muhammad J. Umer[1†], Hao Liu[1], Haifen Li[1], Runfeng Wang[1], Qianxia Yu[1], Shaoxiong Li[1], Rajeev K. Varshney[2], Manish K. Pandey[3], Yanbin Hong[1*], Qing Lu[1*] and Xiaoping Chen[1*]

Abstract

Background Peanuts are important oil crop with an atypical fruitification pattern. Darkness and mechanical stimulation are required to facilitate normal pod development. Despite some progress in understanding peanut pod development and its response to external environmental stimulation, numerous unresolved questions and knowledge gaps remain regarding the role of darkness and mechanical stimulation in this complex process.

Results In this study, we investigated the impacts of dark and mechanical stimulation on peanut pod development via transcriptome. A total of 55,087 genes, along with a series of DEGs and pathways, were identified among different treatment groups (CK, TB, TML, and TMB) that play crucial roles and offer a novel perspective on the role of photosynthesis during peanut pod development. Moreover, by utilizing weighted gene coexpression network analysis (WGCNA) we identified several hub genes (e.g., *IAA9* (*Ahy_B07g086610*), *BSK5* (*Ahy_B03g068305*), *GRF7* (*Ahy_B10g103808*), and *PER17* (*Ahy_B10g105104*)) and key pathways (e.g., plant hormonal and signal transduction pathway, and lignin biosynthesis pathway) that might be true candidates for peanut pod development. Further, the expression patterns of key candidates were validated via qRT-PCR during different pod development stages.

Conclusions Overall, this study provides a comprehensive characterization of the mechanisms underlying peanut pod development in response to darkness and mechanical stimulation. These findings lay a foundation for exploring optimized growth conditions for peanut cultivation, while the identified key genes may serve as potential targets in future peanut breeding programs.

Keywords Peanut, Mechanical stimulation, Environment, Pod development, Gene modules

[†]Lu Huang and Muhammad J. Umer contributed equally to this work.

*Correspondence:
Yanbin Hong
hongyanbin@gdaas.cn
Qing Lu
luqing@gdaas.cn
Xiaoping Chen
chenxiaoping@gdaas.cn

[1]Crops Research Institute, Guangdong Academy of Agricultural Sciences, Guangdong Provincial Key Laboratory of Crop Genetic Improvement, South China Peanut Sub-Centre of National Centre of Oilseed Crops Improvement, Guangzhou, China
[2]WA State Agricultural Biotechnology Centre, Centre for Crop and Food Innovation, Food Futures Institute, Murdoch University, Murdoch, WA, Australia
[3]International Crops Research Institute for the Semi-Arid Tropics (ICRISAT), Hyderabad, India

Introduction

Cultivated peanut (*Arachis hypogaea* L.) is among the most important leguminous crops. By 2022, the global total acreage of cultivated peanuts has reached 30.5 million ha with an annual production of 54.2 million tons (FAO: https://www.fao.org/home/en). Peanut was succ essfully bred for intensive cultivation ~6,000 years ago in South America and is now a global crop cultivated across 100 countries as an essential source of vegetable oil and protein [1, 2]. Compared to other angiosperms, Peanuts exhibit a distinctive reproductive feature known as"geocarpy,"which develops aerial flowers followed by subterranean pods [3]. After fertilization, the activation of intercalary meristem at the base of the ovary leads to the development of a gynophore (peg), which extends to the soil in a positive geotropic manner [4, 5]. After the peg enters the soil, embryo growth and differentiation are resumed, and a seed is produced and begins the maturation process [6]. On the other hand, pegs that failed to penetrate soil became green and lignified pegs that arrest in development [7]. The atypical fructification pattern sets peanuts hold great value for studying organogenesis and evolution and has piqued the interest of researchers [8].

Previous studies have highlighted the role of physiological and environmental factors that influence peanut subterranean fruiting traits. The normal development of peanut pods is believed to be regulated by various plant hormones, including auxin, gibberellin, and ABA, and gynophore elongation was stimulated by a combination of IAA and gibberellin [9–11]. These plant hormones undergo dynamic changes at different growth stages under genetic and environmental factors, leading to phenotypic variation [12–14]. For example, light has been reported to promote the elongation of peanut pegs, and overexposure could, in turn, restrict peanut reproductive development by reducing flower and fruit formation [15, 16]. In contrast, darkness is a necessary factor in inducing fruit formation [10]. Following peg penetration into the soil, fruit expansion commences, accompanied by the cessation of peg elongation. Darkness triggers an irreversible arrest of cell division in the intercalary meristem, and manipulation of light–dark conditions can completely control fruit development [17].

On the other hand, when the peg enters the soil, the mechanical stimulation from the soil on the peg influences its development. The peg tip can respond to external mechanical stimulations, and daily finger touching on the peg tip was reported to induce fruit development and formation [10]. These studies have shed light on the influence of key factors such as darkness and mechanical stimulation on peanut subterranean fruit development. However, this process's specific molecular mechanisms are not yet fully understood.

Studies based on transcriptomics, proteomics, and metabolomics have provided insights into the molecular changes during underground peanut pod development [18–20]. Several studies have revealed that successful pod development in peanuts involves multi-level regulation, including various hormones, gene expression, and signal transduction pathways. After penetration into the soil, the transcriptional level of a large number of genes in gynophore changed significantly, including genes encoding key enzymes for hormone metabolism, photosynthesis, light signaling, cell division and growth, carbon and nitrogen metabolism, as well as genes involved in stress responses [18]. During pod development, Multiple gene sets in the pod wall were enriched for response to various stimulations, including gravity, light, and subterranean environmental factors, suggesting their potential involvement in geocarpy [8, 21].

Furthermore, several studies have attempted to elucidate how key factors, such as darkness and mechanical stimulation, influence peanut pod development. In aerial pods that lacked darkness and mechanical stimulation, there was a significant increase in IAA content, indicating its potential as a crucial factor leading to pod abortion [22]. Transcriptome-based analysis revealed that differentially expressed transcripts were mainly involved in pathways related to photosynthesis, plant-pathogen interaction, DNA replication, and circadian rhythm [23, 24]. The dynamic changes of differentially expressed transcripts in seed and shell found a pronounced enrichment of photosynthetic genes in both the aerial pod and the developing pod under dark conditions [5]. Several genes, including phytochrome A (Phy A), auxin response factor 9 (IAA9), and two senescence-associated genes, have been suggested to be associated with peanut pod abortion [23, 24]. Comparative studies revealed that proteins with different abundance in pods subjected to varying treatments of darkness and mechanical stimulation involved many pathways such as photosynthesis, stress and defense, protein degradation, and lignin synthesis [7, 19].

While previous studies have significantly advanced our understanding of darkness and mechanical stimulation in peanut pod development, these prior investigations still exhibit methodological constraints. Specifically, most existing research could only assess the combined effects of darkness and mechanical stress but failed to isolate individual factors (e.g., technical challenges in maintaining adequate light exposure during sustained mechanical stimulation). Consequently, existing research has yet to clearly delineate the independent impacts of darkness/mechanical stimuli or their synergistic interactions during subterranean pod development.

In this study, to bridge this gap and elucidate the roles of darkness and mechanical stimulation in peanut pod

development, we designed an experiment simulating both individual and combined effects of these stimuli. By applying comparative transcriptome analysis, we systematically identified treatment-specific differentially expressed genes (DEGs) and their associated pathways. Furthermore, through weighted gene co-expression network analysis (WGCNA), we identified several gene modules and hub genes that played pivotal roles in peanut pod development and explored their expression dynamics during different pod development stages. Our findings provide valuable insights into the mechanisms underlying peanut pod development.

Materials and methods

Dark and mechanical stimulation treatments and sample collection

In our study, the peanut cultivar'Yueyou43'was selected as the experimental material. As an erect-plant-type peanut cultivar with high yield (~ 4.5 t/ha), it ensured the availability of sufficient gynophores at synchronized developmental stages for experimental sampling. Moreover, as a widely cultivated variety in southern China, it has demonstrated strong adaptability to the environmental conditions of our experimental station in Guangdong province. On the eighth day after flowering (DAF), each of the selected elongating aerial pegs was stuck into glass tubes for further development. The pegs were then divided into four groups: 1) CK group (No dark or mechanical stimulation, the control group): pegs grown in transparent tubes with no dark or mechanical stimulation; 2) TB group (Dark stimulation only): tubes were wrapped with tinfoil to ensure complete darkness during the development of pegs; 3) TML group (Mechanical stimulation only): transparent tubes were filled with transparent glass beads, which allowed the adequate mechanical stimulation to the pegs without interfering the illumination; 4) TMB group (Dark and mechanical stimulation): tinfoil-wrapped tubes filled with transparent glass beads, which ensured both dark and mechanical stimulation. Each tube was sealed with polyethylene film to prevent rainwater. For each treatment, three biological replicates were performed. After growing for twenty days, a peg from each tube was collected for further analysis. Peanut plants used for the current research were grown in the spring (March- July 2022) at the experimental station of Guangdong Academy of Agricultural Sciences.

RNA extraction and Illumina sequencing

Total RNA was extracted from each peanut pod sample using the TRIzol reagent (Invitrogen) following the manufacturer's instructions. Extracted RNAs were purified using RNase-free DNase I (Qiagen) to remove residual genomic DNA. Ribosomal RNA was removed using the Ribo-Zero rRNA Removal Kit (Illumina). The quality and quantity of the extracted RNA were assessed using a NanoDrop spectrophotometer (Thermo Fisher Scientific) and agarose gel electrophoresis. Only high-quality RNA samples (A260/A280 ratio of 1.8–2.2, OD260/230 ≥ 2.0, RIN ≥ 6.5, 28S:18S ≥ 1.0) were used for further analyses. Sequencing libraries were generated using the NEBNext Ultra Directional RNA Library Prep Kit (New England Biolabs) following the manufacturer's protocol. The libraries were quantified using a Qubit dsDNA HS Assay Kit (Thermo Fisher Scientific) and assessed for quality using a Bioanalyzer 2100 system (Agilent Technologies). Finally, the libraries were pooled in equimolar ratios and sequenced on an Illumina HiSeq4000 platform with 150 bp paired-end reads.

Transcriptome assembly and annotation

Our study followed a standard pipeline to analysis RNA-seq data with replicates [25]. Raw sequencing reads were quality-checked using FastQC (version 0.19.3) and trimmed of adapters and low-quality bases using Trimmomatic (version 0.39) [26]. Clean reads were aligned to the reference peanut genome of *Arachis hypogaea* cv. Fuhuasheng (https://www.ncbi.nlm.nih.gov/data-hub/genome/GCA_004170445.1) using HISAT2 (version 2.2.1) with default parameters [27]. The hierarchical indexing scheme of HISAT2 allows efficient and splice-aware alignment of sequencing reads, which was proved useful in RNA-seq analysis [28]. The mapped reads were then subjected to StringTie (version 2.1.5), which applies network streaming algorithms to assemble and quantitate full-length transcripts (version 2.1.5) [29]. Novel genes were identified by comparing with reference transcript using GffCompare [30] (class code other than"i","u", or"x"). The combined annotation (novel genes + known genes) was then applied for further analysis. We extracted each gene's sequence to annotate the annotated genes'function. We utilized the DIAMOND software to compare them with various databases, including KEGG, GO, NR, Swiss-Prot, TrEMBL, and KOG, using an E-value threshold of 1e-5 [31]. Additionally, we employed iTAK, which integrates PlnTFDB and PlantTFDB, to predict plant transcription factors [32–34].

Differential expression analysis and WGCNA analysis

The FPKM (Fragments Per Kilobase of transcript per Million fragments mapped) values were extracted using featureCounts (version 2.0.1) and utilized to measure the expression levels of each gene [35]. Pearson's correlation coefficient was employed to assess the pairwise correlation of expression profile between samples. The expression matrix was imported into R (version 4.1.0) for differential gene expression analysis using the DESeq2 package (version 1.32.0). DESeq2 employs a negative

binomial distribution model, estimates dispersion and fold change with data-driven prior distributions, thereby ensuring more accurate results in differential expression analysis [36]. Genes with an adjusted p-value < 0.05 and a log2 fold change ≥|1| were considered differentially expressed. These genes were further selected for hypergeometric test-based GO and KEGG enrichment analysis (GO and KEGG) using the clusterProfiler package (version 4.0.5) in R [37]. The co-expression network was constructed using the R package Weighted Gene Co-expression Network Analysis (WGCNA) version 1.72–5 [38]. By using WGCNA we are able to construct a scale-free co-expression network and identifies coordinated gene expression patterns from large scale data. Initially, genes were filtered to exclude those with low expression and low variability between samples. Specifically, genes were required to have a median absolute deviation (MAD) of no less than two and an FPKM (Fragments Per Kilobase of transcript per Million mapped reads) value above 10 in at least 25% of the samples. The network modules were generated using the topological overlap measure (TOM) [39]. The function blockwiseModules was applied to build the network. Highly correlated genes were grouped into modules using average linkage hierarchical clustering, and the minimum size of each module was set to 50. The DynamicTreeCut algorithm was employed to detect co-expression modules, with MergeCutHeight set to 0.15 used to merge modules exhibiting a similarity of 0.75.

For each module, the eigengene was computed using the moduleEigengenes function and subsequently utilized to identify potential relationships with each group. The eigengene-based connectivity value kME and the kME P-values were calculated to infer modular membership. The module eigengene (ME) value was calculated for each module to test the association with phenotype. Mechanical stimulation and darkness were not considered quantitative traits, so they were dichotomized as either present (1) or absent (0). Hub genes for each module were selected using the R package dhga (version 0.1), which is based on the assumption that genes that rank high in connectivity tend to play a more significant role and thus are selected as hub genes [40]. Furthermore, we visualized the coexpression networks of the hub genes from each module and their associated genes to investigate the functional relationships within and between modules.

cDNA synthesis and quantitative real-time PCR

The expression of selected genes was validated using quantitative real-time polymerase chain reaction (qRT-PCR) to confirm their significance. Total RNA was reverse transcribed into cDNA using the PrimeScript RT reagent Kit with gDNA Eraser (Takara Bio). Gene-specific primers were designed using Primer3 (version 2.3.7) and synthesized by a commercial vendor (Supplementary Table S1). qRT-PCR was performed on a StepOnePlus Real-Time PCR System (Applied Biosystems) using the TB Green Premix Ex Taq II (Tli RNaseH Plus) kit (Takara Bio). The 2^(-ΔΔCt) method was used to calculate relative gene expression levels, with the actin-Z gene as the reference gene for normalization. Each measurement was made with three biological replicates and data histograms with means ± SE.

Statistical analysis and visualization

All statistical analyses were performed using R (version 4.1.0). Data were expressed as mean ± standard deviation (SD) of three biological replicates. Student's t-test was used to determine significant differences among groups at a significance level of $p < 0.05$. The weighted gene expression network was visualized by Cytoscape [41].

Results

Phenotypic variations after mechanical stimulation

In the current experiment, the control group (CK) displayed a characteristic aborted phenotype characterized by the absence of swelling at the tip of the peg. In contrast, the TB group, where tubes were wrapped with tinfoil to ensure complete darkness during peg development, and the TML group, where transparent tubes filled with transparent glass beads provided adequate mechanical stimulation without interfering with illumination, both exhibited an aborted phenotype with a slight increase in peg diameter. The TMB group, which used tinfoil-wrapped tubes filled with transparent glass beads to ensure darkness and mechanical stimulation, demonstrated the most pronounced swelling. Both the TB and TMB groups exhibited albino phenotypes due to the lack of light, and all aborted pods showed lignification (Fig. 1A-B).

Transcriptome profiling in response to dark and mechanical stimulation

A total of 55,087 genes, including 9,758 novel genes, were identified in our study (Supplementary Table S2). Sample correlation and PCA analyses revealed strong intra-group similarity, with the most pronounced inter-group divergence observed between CK and TMB (0.71–0.74), followed by CK vs. TB (0.84–0.87) and TML vs. TMB (0.84–0.87) (Fig. 1C-D). Differential expression analysis demonstrated treatment-specific responses, with the CK-TMB comparison showing the most differentially expressed genes (DEGs) (7,143), followed by TML-TMB (4,664) and CK-TML (2,288) (Fig. 1E, Supplementary Table S3). Thirty-two core DEGs were consistently regulated across all comparisons (Fig. 1F), potentially serving as universal regulators of pod development under dark

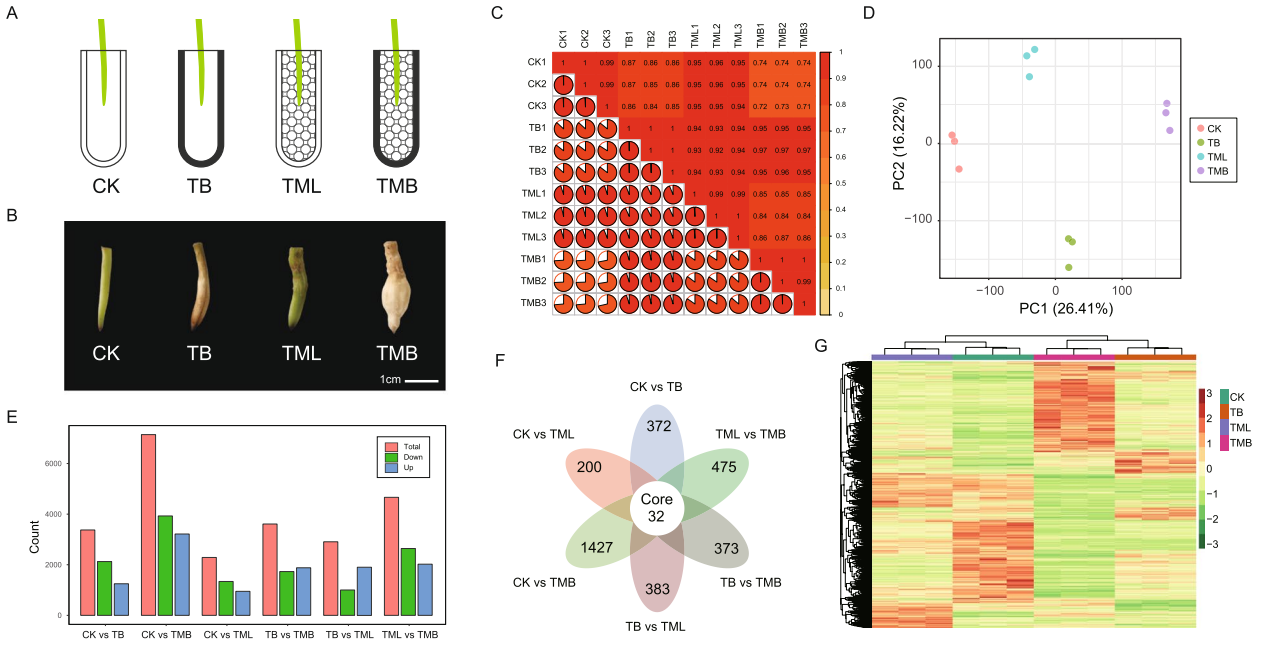

Fig. 1 Experimental design, phenotypes, and transcriptomic landscape across four groups. **A** Different treatments are available in the four groups: CK (No dark or mechanical stimulation), TB (Dark stimulation only), TML (Mechanical stimulation only), and TMB (Dark and mechanical stimulation). **B** Development of pegs under the four treatment groups. **C** Pairwise correlation among samples. **D** Principal Component Analysis (PCA) plot based on the expression matrix of samples. **E** Bar plot illustrating the number of differentially expressed genes and the count of upregulated/downregulated genes between each group. **F** Venn diagram depicting the overlap of differentially expressed genes among the groups and the core genes. **G** Heatmap displaying the clustering of differentially expressed genes across the groups

and mechanical stimuli. Hierarchically clustering further confirmed the high similarity between TB and TMB, as well as between CK and TML (Fig. 1G).

Primary- and secondary- gene sets in response to darkness

To further investigate the synergistic effects of dark conditions and mechanical stimulation on peanut pod development, we conducted additional analysis on the differentially expressed genes (DEG) among all the groups. We defined the intersection of DEGs between CK vs. TMB, CK vs. TB, and TML vs. TMB as DRG1 (dark responsive gene set 1) (Fig. 2A). The subset of DEGs was shared across all comparisons between dark and non-dark conditions, irrespective of whether the peg followed the proper developmental trajectory towards a typically developed pod. Additionally, we selected genes belonging to the CK vs. TMB and TML vs. TMB DEG groups but not included in the CK vs. TB comparison, defining them as DRG2 (dark responsive gene set 2) (Fig. 2A). These genes also exhibited a response to dark stimulation but were explicitly associated with successfully enlarged pods.

We identified 1,341 DRG1 (14.8% of all compared DEGs from CK vs. TMB, CK vs. TB, and TML vs. TMB) genes, which consist of 336 upregulated genes and 987 downregulated genes in response to dark stimulation, respectively. For DRG2, 2,215 (24.4%) genes were identified, including 1,306 upregulated and 915 downregulated genes (Fig. 2B). Subsequent enrichment analysis revealed that DRG1 was significantly enriched in GO terms primarily associated with photosynthesis, with the top five enriched terms being photosystem II, photosystem I, photosynthesis, light reaction, and thylakoid lumen (Fig. 2C) (Supplementary Table S4). The top five enriched KEGG terms for DRG1 were photosynthesis, carbon metabolism, plant hormone signal transduction, glyoxylate metabolism, and phenylpropanoid biosynthesis (Fig. 2D) (Supplementary Table S4). In contrast, the pathway enrichment results for DRG2 were significantly different from DRG1. The top five enriched GO terms for DRG2 were nuclear division, the anchored component of the plasma membrane, regulation of the cell cycle process, mitotic nuclear division, and mitotic cell cycle phase transition (Fig. 2E) (Supplementary Table S4). Furthermore, the top five enriched KEGG terms for DRG2 were plant hormone signal transduction, MAPK signaling pathway, plant-pathogen interaction, DNA replication, and phenylpropanoid biosynthesis (Fig. 2F) (Supplementary Table S4).

Primary- and secondary-responsive gene sets to mechanical stimuli

Following a similar approach to the definition of DRG1 and DRG2, we categorized the DEG dataset into two main groups, MSRG1 and MSRG2. MSRG1 included the DEGs shared between CK vs. TMB, CK vs. TML, and

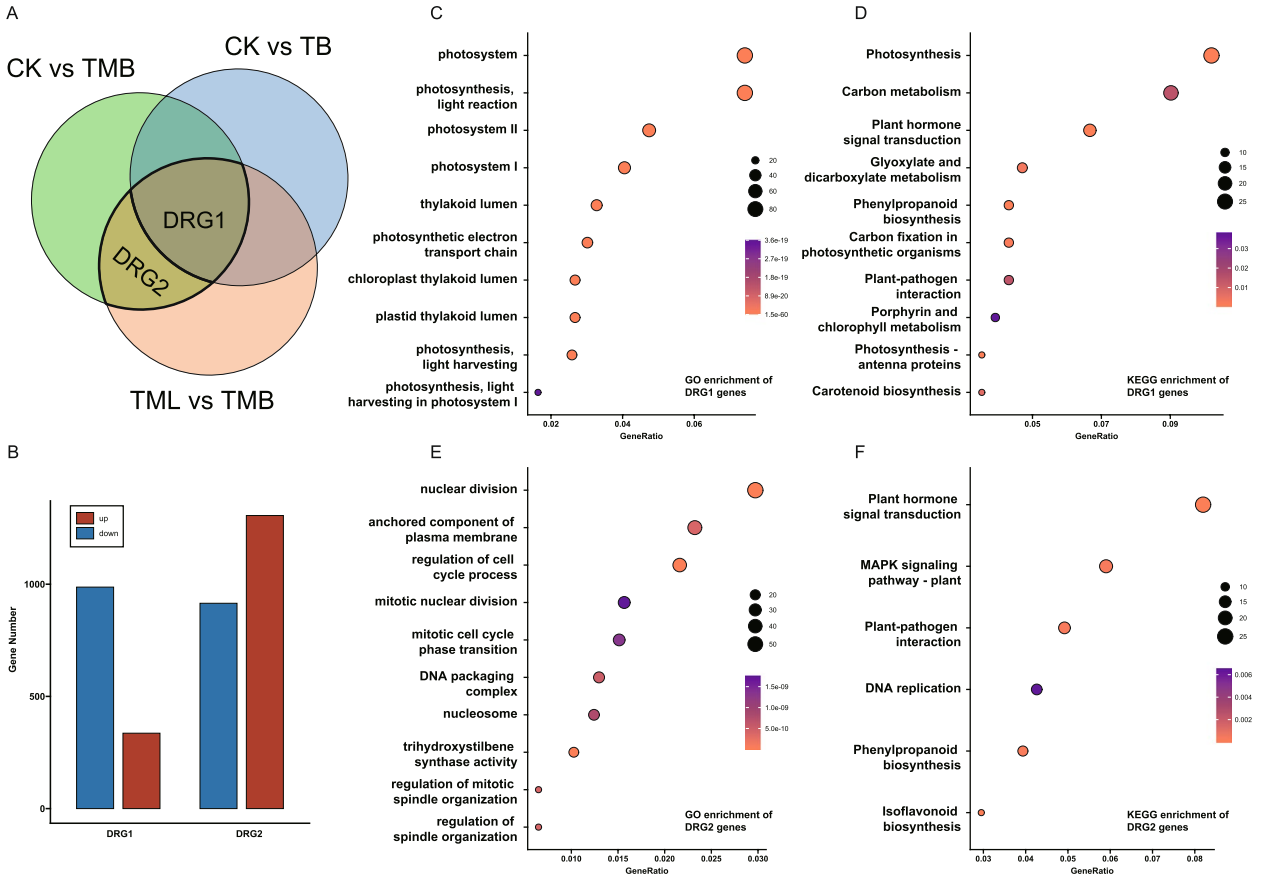

Fig. 2 Primary- and secondary-responsive gene sets to darkness. **A** Venn diagram illustrating the categorization of DRG1 and DRG2 gene sets. **B** Bar plot depicting the number of upregulated and downregulated genes in the DRG1 and DRG2 gene sets. **C** Gene Ontology (GO) bubble plot displaying the enriched GO terms in the DRG1 gene set. **D** Kyoto Encyclopedia of Genes and Genomes (KEGG) bubble plot illustrating the enriched pathways in the DRG1 gene set. **E** GO bubble plot showing the enriched GO terms in the DRG2 gene set. **F** KEGG bubble plot presenting the enriched pathways in the DRG2 gene set

TB vs. TMB, while MSRG2 consisted of DEGs belonging to both CK vs. TMB and TB vs. TMB but not included in the CK vs. TML comparison (Fig. 3A). The rationale behind this categorization was that MSRG1 represented the DEGs differentially expressed between all mechanical and non-mechanical stimuli, regardless of whether the peg underwent enlargement and development. In contrast, MSRG2 precisely captured the genes associated with peg enlargement and development in response to mechanical stimulation.

Seven hundred forty-nine genes (8.7%) were identified as belonging to MSRG1, including 148 upregulated genes and 546 downregulated genes (Fig. 3B). GO pathway enrichment analysis revealed that MSRG1 was primarily enriched in the following five pathways: flavonoid biosynthetic process, flavonoid metabolic process, response to chitin, O-methyl transferase activity, and xenobiotic transmembrane transporter activity (Fig. 3C) (Supplementary Table S5). KEGG pathway enrichment analysis showed that MSRG1 was mainly enriched in the following pathways: Biosynthesis of secondary metabolites, Phenylpropanoid biosynthesis, Plant-pathogen interaction, Plant hormone signal transduction, and MAPK signaling pathway (Fig. 3D) (Supplementary Table S5). On the other hand, 1,958 genes (22.8%) were identified as belonging to MSRG2, including 1,256 upregulated genes and 695 downregulated genes (Fig. 3B). The major enriched GO terms for MSRG2 included microtubule binding, tubulin binding, nuclear division, anchored component of the plasma membrane, and microtubule motor activity (Fig. 3E) (Supplementary Table S5). The main enriched KEGG pathways for MSRG2 included Plant hormone signal transduction, Plant-pathogen interaction, MAPK signaling pathway, Phenylpropanoid biosynthesis, and DNA replication (Fig. 3F) (Supplementary Table S5).

Activation of hormonal signal transduction in response to dark and mechanical stimulation

Plant hormones have been widely reported to be involved in the multi-level regulation of plant responses to stresses, growth, and development. In this study, to elucidate the expression changes of hormone-regulated pathway genes in peanut pegs in response to darkness and mechanical

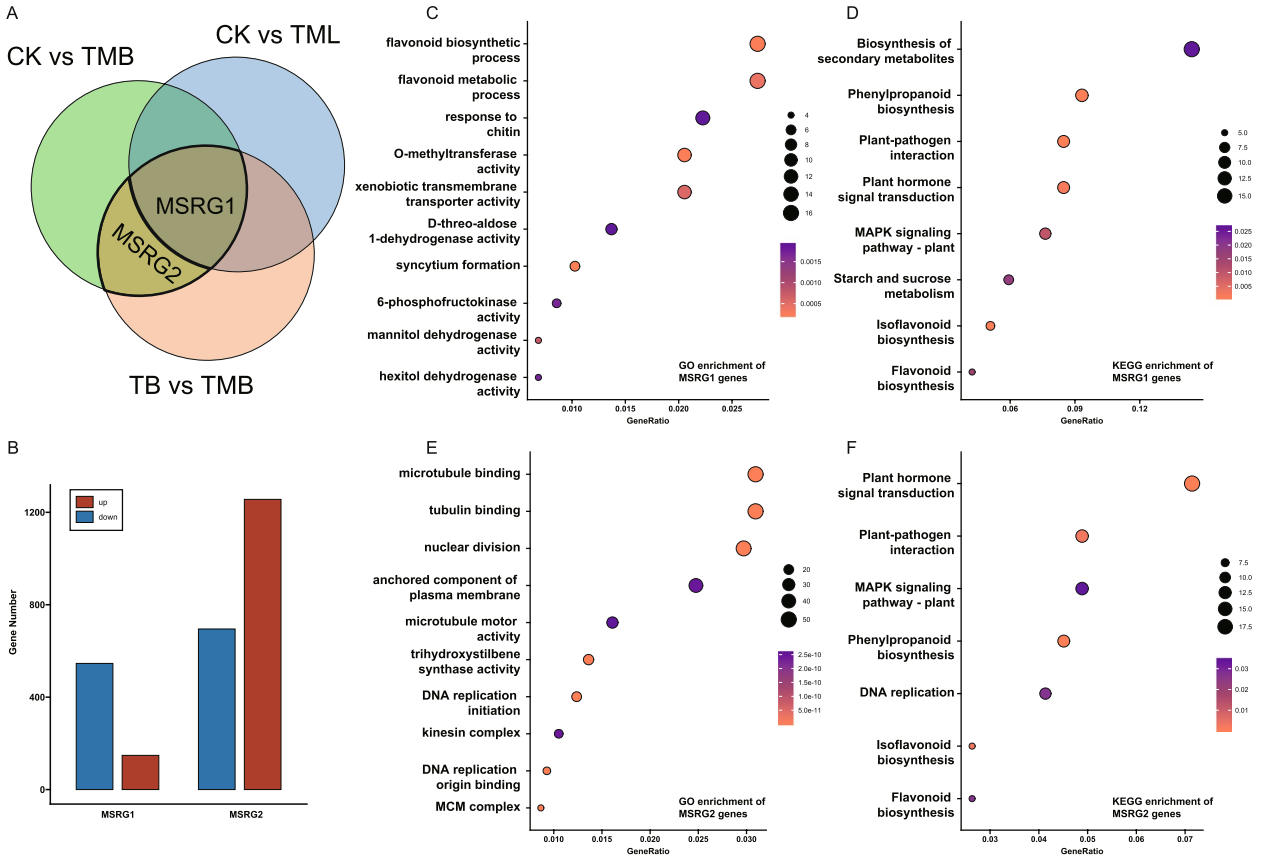

Fig. 3 Primary- and secondary-responsive gene sets to mechanical stimulation. **A** Venn diagram illustrating the categorization of MSRG1 and MSRG2 gene sets. **B** Bar plot depicting the number of upregulated and downregulated genes in the MSRG1 and MSRG2 gene sets. **C** Gene Ontology (GO) bubble plot displaying the enriched GO terms in the MSRG1 gene set. **D** Kyoto Encyclopedia of Genes and Genomes (KEGG) bubble plot illustrating the enriched pathways in the MSRG1 gene set. **E** GO bubble plot showing the enriched GO terms in the MSRG2 gene set. **F** KEGG bubble plot presenting the enriched pathways in the MSRG2 gene set

stimulation, we selected differentially expressed genes (DEGs) between different groups. We compared them with previously reported genes involved in plant signal transduction. Heatmap analysis was used to display the expression trends of DEGs across different groups (Fig. 4). Results from the auxin pathway showed a general upregulation of *ARF* (Auxin Response Factor) genes in peanut pegs under dark stimulation. Three *IAA9* genes (*Ahy_A03g011227, Ahy_A07g033338,* and *Ahy_A08g038618*) exhibited significant upregulation in samples subjected to dark stimulation. In the Jasmonic acid signaling pathway, we observed significant expression changes in several differentially expressed genes (DEGs). Among them, the *JAZ* (Jasmonate ZIM-domain) genes (*Ahy_B01g056302* and *Ahy_A01g000588*), the central repressors in the jasmonic acid signaling cascade, exhibited a significant upregulation trend in the TMB group, contrasting with its relatively lower expression in the CK and TML groups. Additionally, the *MYC2* genes showed a significant upregulation in the TMB group. These results suggest that the jasmonic acid signaling pathway genes undergo significant expression regulation in peanut pegs responding to darkness and mechanical stimulation. Moreover, the brassinosteroid (BR) signaling pathway also showed expression changes in some differentially expressed genes (DEGs). In the dark and mechanical stimulation samples, several BR synthesis-related genes exhibited a significant upregulation trend, while they were relatively lower in the other three groups. These genes include six *BRI1* (Brassinosteroid Insensitive 1) genes (*Ahy_A02g006564, Ahy_B02g061362, Ahy_B01g053256, Ahy_A03g015928, Ahy_B03g067395,* and *Ahy_B05g079759*), two *BSK* (Brassinosteroid-Signaling Kinases) genes (*Ahy_B03g068305*, and *Ahy_A03g016701*), and two *CYCD3* genes (*Ahy_B06g085978*, and *Ahy_A06g030901*). In comparison, the expression levels of four TCH4 genes (Ahy_A01g001492, Ahy_B01g054999, Ahy_B03g065721, and Ahy_A01g001599) were consistently higher in the control group (CK) compared to the other groups, with the TMB group exhibiting the lowest expression across all treatments. These findings suggest that the brassinosteroid signaling pathway may play a crucial regulatory role in peanut pod development under dark and mechanical stimulation, potentially modulating this response through mechanisms that promote cell division rather than elongation.

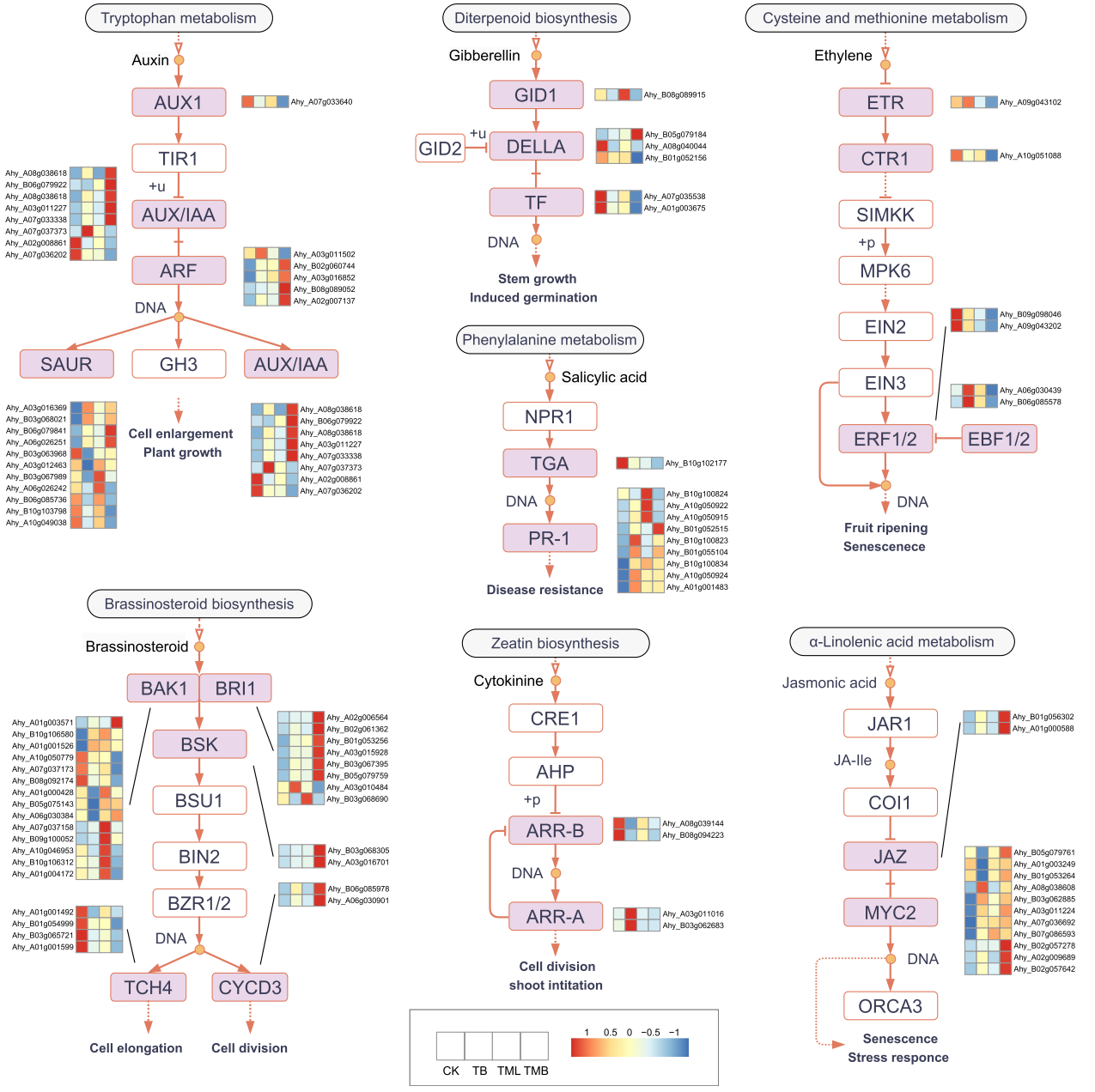

Fig. 4 Differentially expressed genes in various plant hormone signaling pathways. Only genes with FPKM values greater than 10 in at least one sample are shown. Pathways without differentially expressed genes are not displayed in the figure. Each row of the heatmap represent one DEG. The four boxes of each row represent CK, TB, TML, and TMB group, respectively. The color scale indicated low (blue) and high expression (red). The gene expression values for each group were the average of three replicated and were z-score normalized among four groups

Expression patterns of genes linked to the biosynthesis of lignin in peanut pods in response to dark and mechanical stimulation

Lignin is one of the main components of peanut shells, which serve as a protective organ to ensure the normal development of seeds and directly influence the size of the pod [42]. According to the enrichment analysis of differentially expressed genes, genes associated with light and dark stimulation were enriched in the phenylpropanoid biosynthesis (ko00940) pathway, indicating its significant role in peanut pod development and enlargement. The products of this pathway, monolignols, undergo oxidative polymerization reactions to form lignins, catalyzed by enzymes such as phenylalanine ammonia-lyase (*PAL*), cinnamic acid 4-hydroxylase (*C4H*), 4-coumarate: CoA ligase (*4CL*), cinnamoyl-CoA reductase (*CCR*), cinnamyl alcohol dehydrogenase (*CAD*), ferulic acid 5-hydroxylase (*F5H*), and caffeic acid O-methyltransferase (*COMT*). Lignin is crucial in plant

growth and development, particularly in forming and lignifying secondary cell walls.

Current results indicated a significant enrichment of differentially expressed genes in the phenylpropanoid biosynthesis pathway among the four groups (Fig. 5). *PAL*, *CCR*, *CAD*, *F5H*, and *COMT* genes showed consistent trends, with generally lower expression levels in the TMB group, suggesting downregulation of genes involved in lignin synthesis as peanut pods experience darkness and mechanical stimulation. Among them, the *PAL* gene exhibited significantly higher expression in the CK and TB groups than in the TML and TMB groups, indicating its potential response to mechanical stimulation.

Weighted gene co-expression network analysis revealed the hub genes linked to peanut pod development

A co-expression network was constructed using 9248 differentially expressed genes. This study chose the soft-threshold power (β) of 19 to ensure a scale-free network. Based on average linkage hierarchical clustering, 17 modules were identified (Fig. 6A, B) (Supplementary Figure S1) (Supplementary Table S6). Among these, three modules—blue, magenta, and green-yellow—showed significant correlations with specific experimental conditions, highlighting their biological relevance.

The blue module (1112 genes) exhibited the strongest positive correlation with the TMB group, as well as the highest proportion of upregulated DRG2 and MSRG2 genes, indicating its activation in response to darkness combined with mechanical stimulation (Fig. 6B, C, D). The magenta module (351 genes) also showed a strong positive correlation with TMB (Fig. 6B, E, F). In contrast, the green-yellow module (275 genes) displayed the highest negative correlation with the TMB group, suggesting its suppression under the same conditions (Fig. 6B, G, H).

For treatments involving single stimuli, the red module (449 genes) correlated most positively with the TML group, while the green module (594 genes) had the highest positive correlation with the TM group, indicating

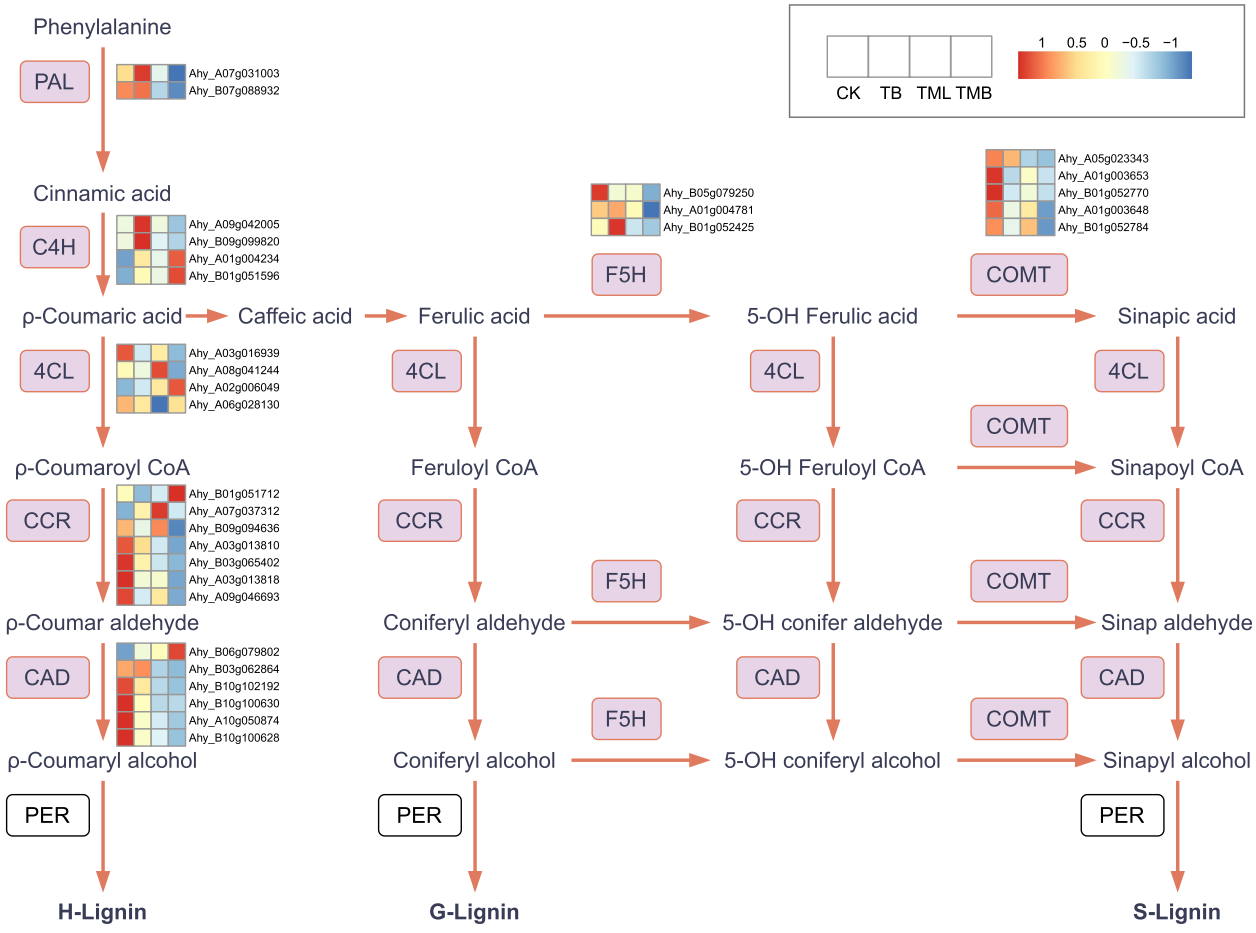

Fig. 5 Differentially expressed genes in phenylpropanoid biosynthesis pathway. Only DEGs with FPKM values greater than 10 in at least one sample are shown. Each row of the heatmap represent one DEG. The four boxes of each row represent CK, TB, TML, and TMB group, respectively. The color scale indicated low (blue) and high expression (red). The gene expression values for each group were the average of three replicated and were z-score normalized among four groups

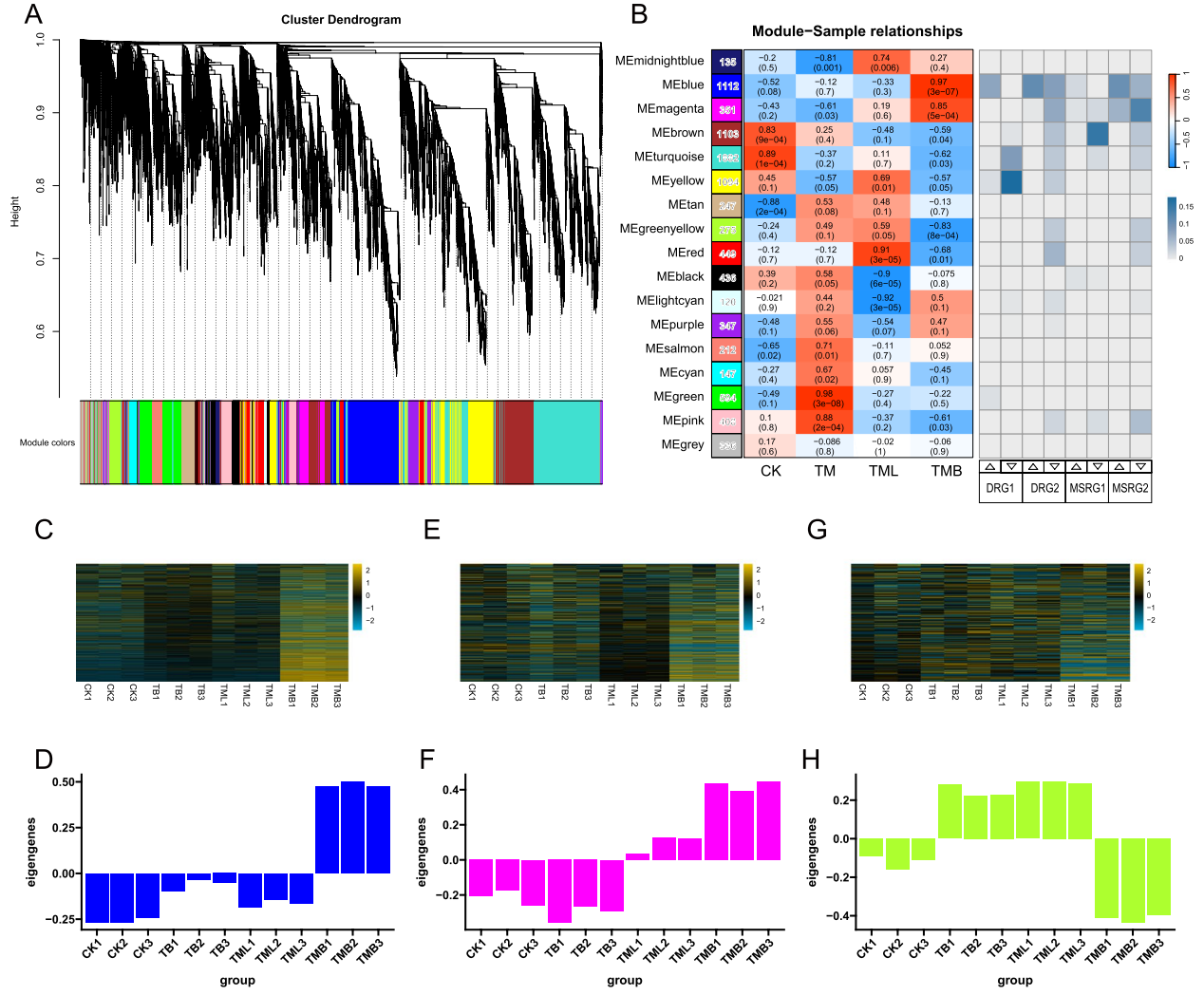

Fig. 6 Weighted gene co-expression network analysis (WGCNA) during peanut pod development. **A** Hierarchical cluster diagram of coexpression modules identified by WGCNA. **B** Module-trait relationships (left) and the overlap of genes from each module with DRGs and MSRGs (right). The numbers within the left heatmap represent Pearson correlations and p-values (in parentheses: red, positively correlated, blue, negatively correlated). The color in the right heatmap represents the number of shared genes with DEG/MSRG as a percentage of the total number of genes per module; the upper and lower triangles represent up-regulated DEGs and down-regulated DEGs, respectively. **(C-H)** The expression profile of blue (**C**, **D**), magenta (**E**, **F**), and green-yellow (**G**, **H**) modules, respectively. **C**, **E**, **G** The expression of the gene set was presented in a heatmap, and (**D**, **F**, **H**) the eigengene values were presented in histograms

their specific activation under darkness or mechanical stimulation alone (Fig. 6B).

We identified the top 25 hub genes from the blue, magenta, and green-yellow modules (Fig. 7A-C). These three modules all demonstrate a significant correlation between module membership and gene significance, while also showing close interconnections among the modules (Fig. 7D, Supplementary Figure S2). In the blue module, we observed several genes associated with plant hormone pathways, such as the *IAA9* (*Ahy_B07g086610*), *BSK5* (*Ahy_B03g068305*), and *MYC2* (*Ahy_B02g057278*) (Fig. 7A). *IAA9* encodes the Auxin-responsive protein IAA9, which plays a pivotal role in auxin-mediated growth and development processes. ***BSK5***, encoding BR-signaling kinase 5, is involved in brassinosteroid signaling, a pathway essential for promoting plant growth and development. Meanwhile, ***MYC2*** encodes a transcription factor that regulates jasmonic acid signaling, a crucial mechanism for plant defense responses and developmental regulation. Notably, all these genes exhibited significantly higher expression levels in the TMB group, highlighting their potential roles in the observed phenotypic responses (Fig. 8). In addition, the hub gene network also revealed two expansin genes, *EXPA6* (*Ahy_A03g016738*) and *EXPA8* (*Ahy_B10g104132*), and a phenylpropanoid biosynthesis-related gene, *PER17* (*Ahy_B10g105104*). These genes showed lower expression levels in the non-swollen development group, suggesting

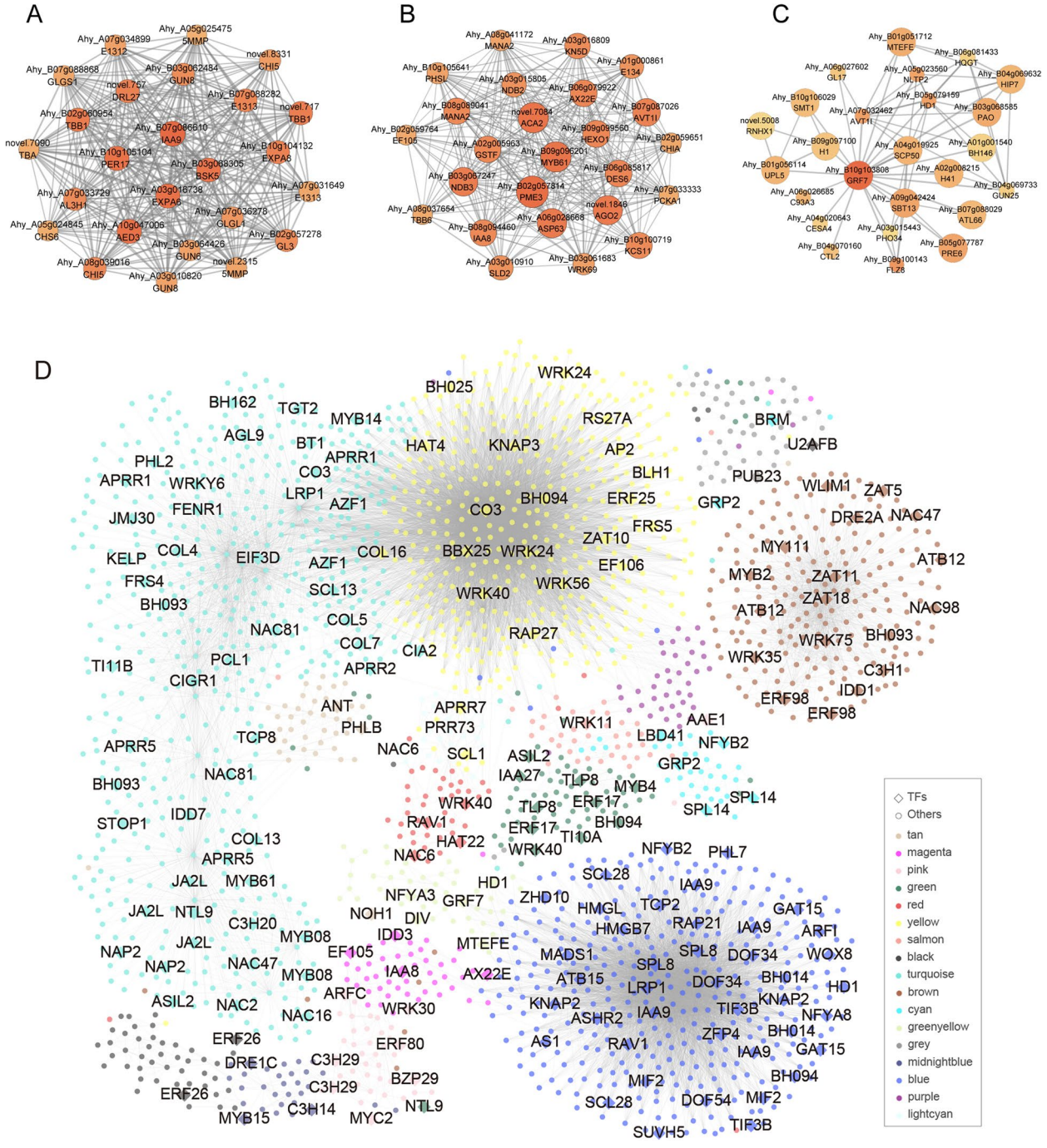

Fig. 7 Coexpression networks and key candidate genes involved in peanut pod development identified by WGCNA. **(A-C)** Cytoscape visualizes the gene correlation networks of the blue (**A**), magenta (**B**), and green-yellow (**C**) modules. Twenty-five hub genes of each module identified by dhga v1.0 were presented. Node size and color are proportional to the number of edges with other genes. **D** Coexpression network showing the hub genes and their associated genes from the 17 modules. The related genes were selected for each hub gene with the following criteria: connectivity weight value threshold > 0.3 or the three associate genes with the highest connectivity weight value (when less than three genes pass the threshold). Gene names of transcription factors are shown in the figure

that their lack of activation may be a crucial factor contributing to pod abortion (Fig. 8).

The hub genes in the magenta module include several genes involved in key biological pathways (Fig. 7B). For instance, *ACA2* (*novel.7084*) encodes an ER-resident protein influenced by calcium-dependent protein kinase, potentially impacting calcium signaling and homeostasis [43]. *MYB61* (*Ahy_B09g096201*) encodes the transcription factor that regulates cellulose synthesis, a factor selected during rice domestication [44]. *PME3*

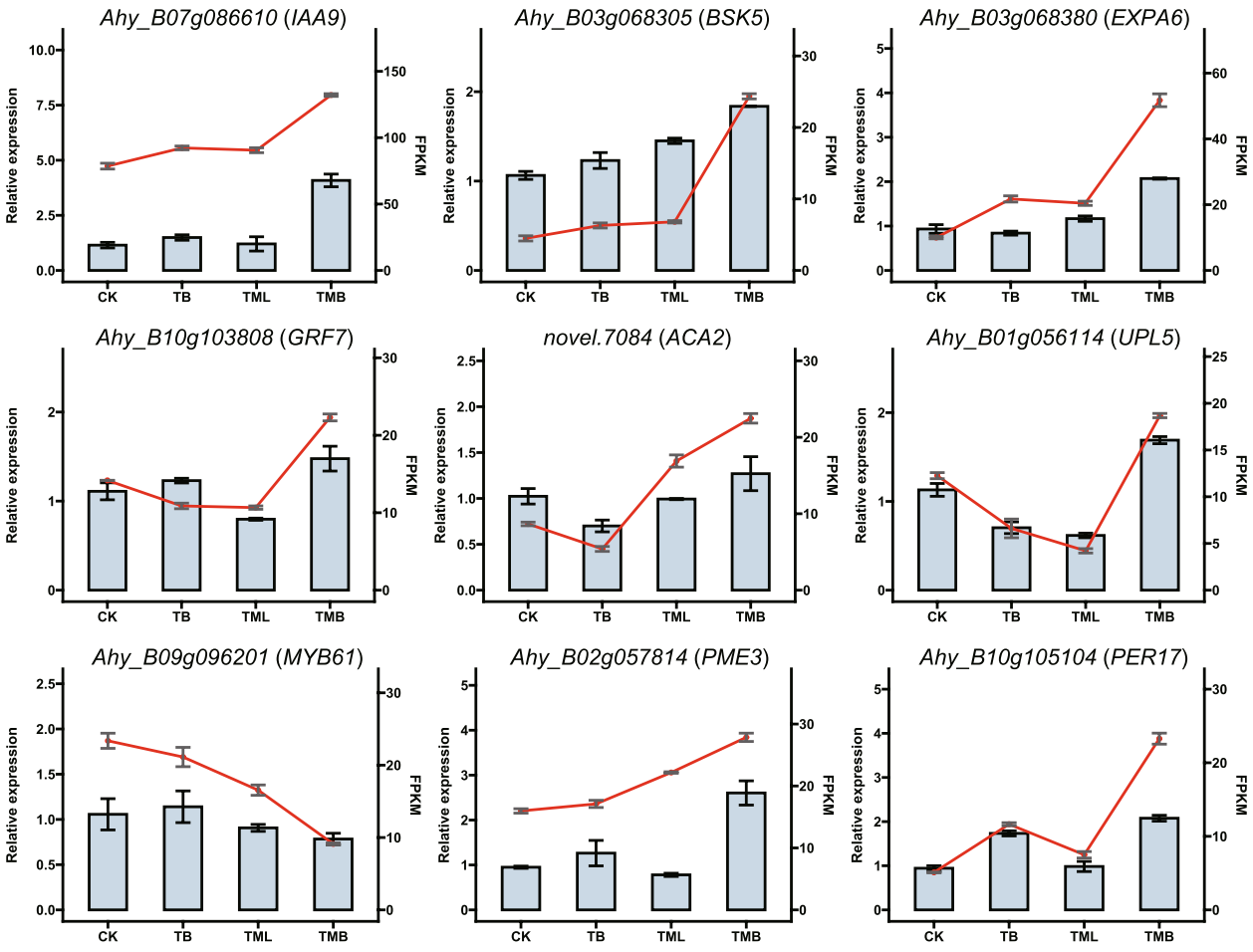

Fig. 8 Expression dynamics of the selected hub genes in the three modules via qRT-PCR for their roles in peanut pod development. The X-axis on the left presents the relative expression, whereas the left x-axis shows the RNA-seq data in FPKM form. Error bars indicate SE obtained from three biological replicates

(*Ahy_B02g057814*) is a major basic isoform of the PME gene in A. thaliana, encoding a ubiquitously expressed cell wall pectin methylesterase. PME3 knockout leads to a distinct phenotype characterized by earlier germination and reduced root hair production [45]. Additionally, this knockout results in downregulating pectin-degrading enzymes and enzymes involved in lipid and protein metabolism in the hypocotyl of 4-day-old dark-grown mutant seedlings [45, 46].

A *GRF7* gene (*Ahy_B10g103808*) was identified at the central position of the green-yellow module, encoding a growth-regulating factor induced by *BZR1* and *PIF4* to repress chlorophyll biosynthesis and promote seedling greening. The suppression of *GRF7* could result in protochlorophyllide accumulation in the dark and severe photobleaching upon light exposure (Fig. 7C). *UPL5* (*Ahy_B01g056114*), another hub gene from the green-yellow module, encodes a HECT-type ubiquitin ligase. Studies have shown that *UPL5* can ubiquitinate *WRKY53*, a key regulatory transcription factor of plant aging and immunity, and is involved in pathogenic responses [47].

Expression patterns of candidate genes via qRT-PCR

To validate the precision and dependability of the RNA-seq data, a set of nine key hub genes (gene with high connectivity with other hub genes), including *IAA9* (*Ahy_B07g086610*), *Ahy_B03g068305* (*BSK5*), *EXPA6* (*Ahy_B03g068380*), *GRF7* (*Ahy_B10g103808*), *ACA2* (*novel.7084*), *UPL5* (*Ahy_B01g056114*), *MYB61* (*Ahy_B09g096201*), *PME3* (*Ahy_B02g057814*), and *PER17* (*Ahy_B10g105104*) was selected for qRT-PCR validation. Consistent with those used for RNA-seq, three peanut pods from each of the four groups were subjected to qRT-PCR analysis. The expression patterns of these genes, as detected by both RNA-seq and qRT-PCR, exhibited remarkable concordance, with a significant correlation coefficient of 0.81 observed between the two methodologies (Fig. 8) (Supplementary Figure S3). Interestingly, we

observed that almost all the genes have higher expression patterns, specifically in the TMB group.

Expression dynamics of key hub genes across the development stages of peanut seeds/shells

Furthermore, we investigated the dynamic changes in the expression patterns of key hub genes during peanut pod development utilizing the previously published data from our group [8]. The expression of key hub genes in peanut seeds and shells at different stages from P0 to P10 was explored (Fig. 9). The results revealed a general trend of high expression during the early stages of expansion (P2-P4), followed by a gradual decrease in expression as maturity progressed. Interestingly, the expression of *IAA9* exhibited synchronous changes in both seeds and shells during pod development and maturation. On the other hand, *BSK5*, *PER17*, and *PME3* exhibited higher expression levels in shells than in seeds. However, we also observed some unique expression patterns. For instance, *EXPA6* displayed a stable high expression in shells (P2-P7), associated with its role in promoting fruit shell expansion. The expression of *GRF7* showed a rapid decline in shells during pod growth and development, while in seeds, it exhibited higher expression levels at the later stages of development (P7-P10).

Discussion

The unique reproductive mode of peanuts has long attracted attention from researchers. The elucidation of the molecular mechanisms underlying peanut pod development and its response to external environmental stimulations has been a significant focus of peanut research. It serves as a key factor in enhancing future peanut production and invaluable material for studying the diversity of reproductive development. In our study, we conducted transcriptomic analysis on peanut pods subjected to treatment combinations of darkness and mechanical stimulation to understand the mechanisms involved in peanut pod development. Unlike conventional approaches that employed aberrant gynophore development (subterranean unswollen pegs and early swelling pods) or daily clamping on the tip [19, 48], we utilized transparent glass balls to treat the gynophore, thereby enabling the simultaneous application of mechanical stimulation while maintaining light exposure, and thus facilitating the isolated investigation of peanut pod responses to mechanical stimulation. Moreover, apparent phenotypic differences were observed in response to darkness and mechanical stimulation (Fig. 1A-B), suggesting deeper insights into any molecular and genetic regulation of pod development.

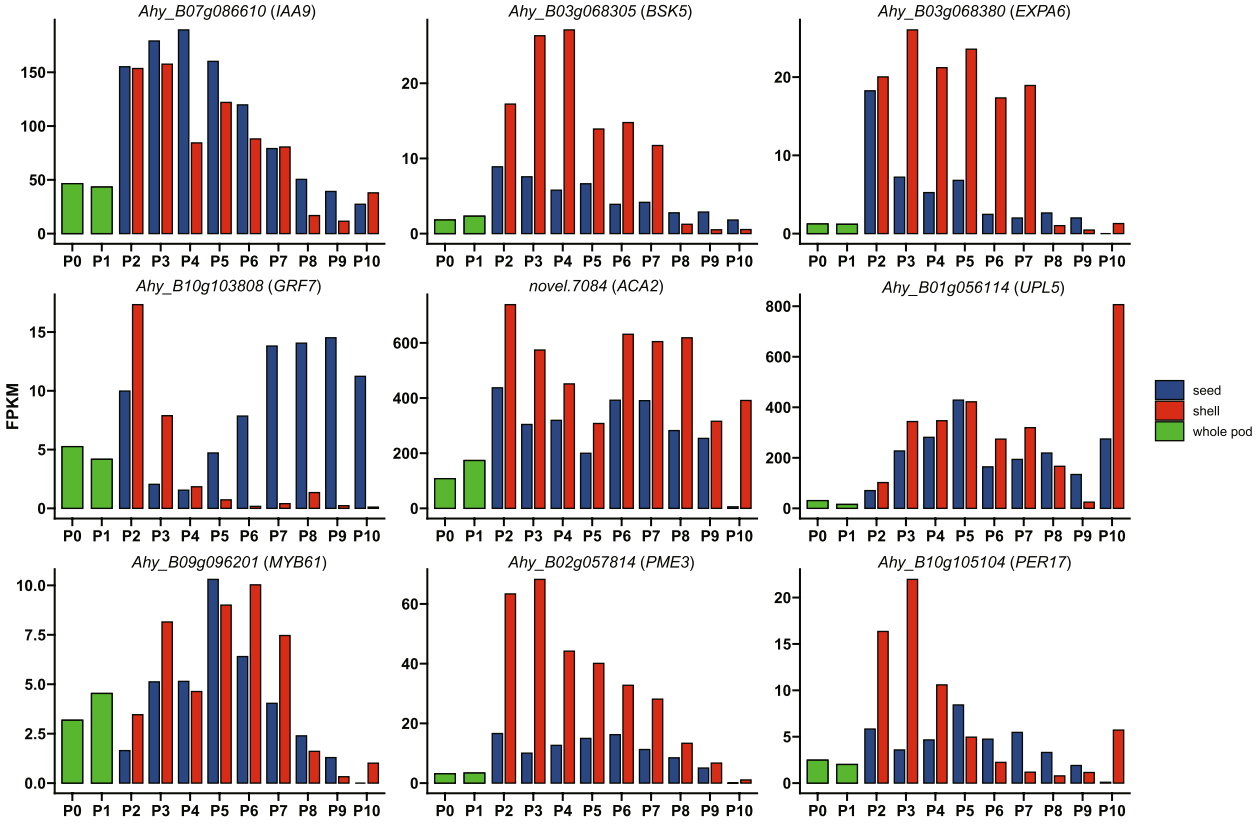

Fig. 9 Analysis of the expression dynamics of key hub genes across 10 development stages of peanut pod. P0 and P1 data were based on whole pod samples

So, we observed the most significant differences in gene expression between the CK and TMB groups by transcriptome profiling and differential expression analysis. Notably, many of these differentially expressed genes (DEGs) were not identified in other comparisons, suggesting that the transcriptional profile of peanut pod development underwent unique changes. We defined these genes as DRG and MSRG according to the study design, where DRG1/MSRG1 denotes DEGs universally associated with darkness and mechanical stimulation, and DRG2/MSRG2 represents DEGs that are not only related to darkness and mechanical stimulation but also correlated with peanut pod expansion.

Among these DEGs, we observed that DRG2 and MSRG2 were enriched in cell division and DNA replication-related GO terms, which was not observed in DRG1 and MSRG1. This suggests that pod swelling results from the coordinated action of darkness and mechanical stimulation. Furthermore, our analysis revealed that several pathways, including phenylpropanoid biosynthesis, plant hormone signal transduction, plant-pathogen interaction, and MAPK signaling pathway, were enriched in both DRG and MSRG. When examining the expression trends, we found that DRG1/MSRG1 genes tend to exhibit negative modulation of gene expression, with most differentially expressed genes (DEGs) displaying decreased expression levels, whereas DRG2/MSRG2 genes exhibit positive modulation of gene expression, with over half of the genes showing increased expression levels. This suggests that the activation/inhibition of key genes in these pathways may be crucial for peanut pod development.

In this study, several pathways exhibited significant activation or suppression in response to darkness and mechanical stimulation (Fig. 4). For example, the auxin, brassinosteroid, ethylene, and jasmonic acid signaling pathways, which are well-established regulators of fruit development in plants, were found to be involved in peanut pod development [49–51]. Previous studies have shown that peanut pod development is accompanied by the regulation of a variety of hormones, including auxin, gibberellic acid (GA), cytokinin, ethylene, and abscisic acid (ABA) [3, 4, 11, 17, 52, 53]. Notably, the co-upregulation of auxin-responsive genes (e.g., *ARF*, *IAA9*) and brassinosteroid (BR) signaling genes (e.g., *BRI*, *BSK5*, *CYCD3*) suggests synergistic and interdependent interactions between these pathways in the regulation of cell division during peanut pod development. Such synergy has been previously observed, as demonstrated by the reduced sensitivity of auxin mutants iaa3 and arf6/arf8 to brassinosteroid for hypocotyl elongation compared to wild-type plants [54]. Additionally, the jasmonic acid pathway was also observed to be significantly activated in the TMB group. Previous studies have demonstrated that its precursor is involved in proper seed development [55]. Moreover, as a pathway that plays an important role in plant responses to both biotic and abiotic stresses, the activation of jasmonic acid signaling pathway may represent a unique adaptation mechanism for pod development in soil environments.

Among these hormone pathway genes, multiple of them played central roles in gene co-expression modules. For example, *IAA9* (*Ahy_B07g086610*) was identified as a hub gene in the WGCNA analysis, with all four copies located in the blue module (Fig. 7A, D). This finding aligns with previous reports that *IAA9* is upregulated upon gynophore penetration, suggesting its critical role in peanut pod swelling [24]. *BSK5* (*Ahy_B03g068305*) has been identified as a hub gene in the blue module and is widely involved in the plant's immune response and hypocotyl elongation [56]. A previous study revealed that the promoter of BSK5 contains a G-box element 3.5 kb from ATG, which can bind multiple phytochrome-interacting factors (PIFs), and the upregulation of *BSK5* was required in the hypocotyl elongation of *Arabidopsis* [57, 58]. Given the crucial roles of these genes and their associated pathways in peanut pod development, specific activation of these genes or pathways may represent promising agricultural targets for enhancing seed development in peanut breeding.

In addition, upon exposure to darkness and mechanical stimulation, many genes involved in the phenylpropanoid biosynthesis pathway were down-regulated in gynophore, including phenylalanine ammonia-lyase (*PAL*), cinnamoyl-CoA reductase (*CCR*), cinnamyl alcohol dehydrogenase (*CAD*), ferulic acid 5-hydroxylase (*F5H*), and caffeic acid O-methyltransferase (*COMT*). Lignin is a complex heterogeneous polymer derived from three monolignols (pcoumaryl, coniferyl, and sinapyl alcohol) [42]. It provides rigidity and hydrophobicity to plant cell walls, facilitates the transport of minerals through the vascular bundles, and serves as a vital barrier against pests and pathogens, thus playing a crucial role in plant growth and development [59–63]. Phenylpropanoid biosynthesis (ko00940) has been reported as the most critical pathway affecting pod development, as the growth rate of pod size was negatively correlated with p-coumaryl alcohol (the precursor of H-type lignin), and peanut varieties with small pod showed significantly less accumulation of p-coumaryl alcohol (H-lignin) [42]. However, whether early lignification contributes directly to the abortion of peanut pods or is merely the byproduct of a rewired metabolism network remains to be explored.

Significantly, a large proportion of genes within DRG1 were found within photosynthesis pathways (Fig. 2C, D), consistent with previous studies. Previous comparative analysis of aborted/early-staged pods to subterranean ones revealed a large proportion of the metabolites/genes

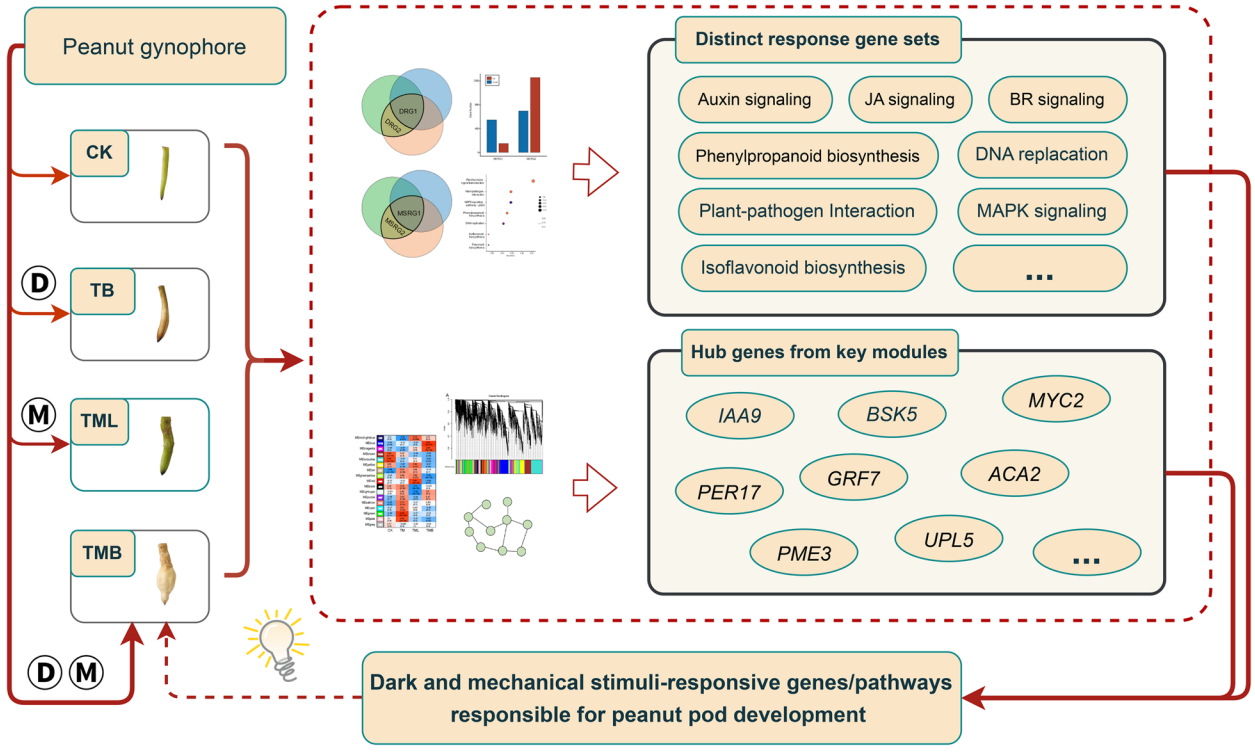

Fig. 10 Schematic diagram summarizing dark and mechanical stimuli-responsive genes/pathways responsible for peanut pod development. Circled capital letter D and M represent darkness and mechanical stimulation, respectively

are enriched in photosynthesis-related pathways, thereby leading to the conclusion that these pathways play a crucial role in peanut pod development [3, 7, 18, 22, 23]. In contrast to DRG1, the enrichment of photosynthesis pathways was not observed in DRG2, and the albino phenotype caused by downgraded photosynthesis pathway genes does not necessarily lead to the pods'swelling (see group TB). Our results imply that the photosynthesis pathway is not (at least directly) linked to peanut pod development. Meanwhile, it is essential to acknowledge the pivotal role of photoreceptor phytochromes (e.g., *PHYA*, *CRY2*, and *CRY3*) in the process of skotomorphogenesis, as the treatment of far-red and darkness can induce pod development by suppressing peg elongation [4, 5]. It is necessary to investigate further the roles of the mechanisms by which these photoreceptors respond to light signals and trigger downstream pathways related to pod swelling.

Our study does have certain limitations. While our glass tube system successfully mimicked the darkness and mechanical stimulation in subterranean conditions (Fig. 10), this controlled environment inherently simplified natural soil complexity. Notably, the absence of certain external factors, such as calcium, moisture, and aeration—may have influenced signaling pathways dependent on these factors [64, 65]. For instance, calcium signaling, which plays a pivotal role in plant growth and development processes, could be dysregulated without natural soil mineral profiles [66]. To address these limitations, future studies could consider incorporating soil-derived solutions to better approximate in situ biochemical interactions.

Nevertheless, this study provides valuable insights into the intricate molecular mechanisms governing peanut pod development, notably highlighting the synergistic effects of darkness and mechanical stimulation. These revelations offer valuable implications for the advancement of peanut breeding strategies and agricultural practices. By utilizing gene editing tools such as CRISPR/Cas9 to target key pathways and hub genes (e.g., *IAA9, BSK5, GRF7, PER17*), there is potential in the future to mitigate gynophore abortion in peanuts due to overexposure to light or the lack of mechanical stimulation, consequently leading to an increase in peanut yield. Further validations and focused research efforts are crucial to translate these discoveries into actionable strategies that could substantially benefit peanut production and agricultural sustainability.

Conclusion

In this study, we simulated underground environments to investigate the effects of darkness and mechanical stimulation on peanut pod development

and characterized the transcriptome profiles of gynophores under each treatment. Through comparative transcriptomic analysis, we identified several hub genes (e.g., *IAA9* (*Ahy_B07g086610*), *BSK5* (*Ahy_B03g068305*), *GRF7* (*Ahy_B10g103808*), and *PER17* (*Ahy_B10g105104*)) and key pathways (e.g., plant hormone signaling pathways and phenylpropanoid biosynthesis pathway) that play pivotal roles in peanut pod development. Our comparative analysis offers a novel perspective on the role of photosynthesis pathway during peanut pod development. Moreover, we identified three co-expression gene modules correlated with peanut pod swelling, validated the expression of hub genes, and explored their expression across different peanut development stages. Our work highlights the synergistic role of darkness and mechanical stimulation and provides valuable insights into peanut pod development mechanisms. These findings have substantial implications for future research and practical applications. For example, functional validation of the identified hub genes through gene editing approaches (e.g., CRISPR/Cas9) will be useful to precisely determine their roles in pod development. From an applied perspective, a deeper understanding of the interplay between darkness and mechanical stimulation in peanut pod development could provide valuable insights for optimizing growth conditions, in controlled environments and field settings. Furthermore, targeting the identified hub genes in breeding programs offers potential for developing cultivars with enhanced stress tolerance and superior pod quality, improving peanut farming productivity and sustainability, thereby contributing to the improvement of productivity and sustainability in peanut farming.

Abbreviations

PAL	Phenylalanine ammonia lyase
CCR	Cinnamoyl-CoA reductase
CAD	Cinnamyl alcohol dehydrogenase
F5H	Ferulic acid 5-hydroxylase
COMT	Caffeic acid O-methyltransferase
C4H	Cinnamic acid 4-hydroxylase
4CL	4-Coumarate: CoA ligase
JAZ	Jasmonate ZIM-domain
ARF	Auxin response factor
DEGs	Differentially expressed genes
KEGG	Kyoto Encyclopedia of Genes and Genomes
GO	Gene Ontology
DRG2	Dark responsive gene set 2
DRG1	Dark responsive gene set 1
PCA	Principal component analysis
CK	Control
SD	Standard deviation
qRT-PCR	Quantitative real-time polymerase chain reaction
WGCNA	Weighted gene co-expression network analysis
FPKM	Fragments per kilobase of transcript per million mapped reads
MAD	Median absolute deviation
DAF	Days after flowering

Supplementary Information

The online version contains supplementary material available at https://doi.org/10.1186/s12870-025-06880-5.

Supplementary Material 1. Supplementary Table S1 Primers used in qRT-PCR.

Supplementary Material 2. Supplementary Table S2 Information on all genes identified in the study, including FPKM values, locations, and gene annotations.

Supplementary Material 3. Supplementary Table S3 Information on all DEGs, including FPKM values, locations, and gene annotations.

Supplementary Material 4. Supplementary Table S4 GO and KEGG annotation results for DRG1 and DRG2 gene sets.

Supplementary Material 5. Supplementary Table S5 GO and KEGG annotation results for MSRG1 and MSRG2 gene sets.

Supplementary Material 6. Supplementary Table S6 The relationship between genes and modules.

Supplementary Material 7. Supplementary Figure S1 Clustering dendrogram (A) and correlation heatmap (B) of modules identified by weighted gene coexpression network analysis.

Supplementary Material 8. Supplementary Figure S2 Scatter plot of module membership vs. gene significance in blue (A), magenta (B), and green-yellow (C) modules. Module membership presents the correlation between gene expression and each module eigengene. Gene significance represents the association between gene expression and each trait.

Supplementary Material 9. Supplementary Figure S3 Fold change correlation between qRT-PCR and RNA-seq data.

Acknowledgements

We want to thank the Crops Research Institute, Guangdong Academy of Agricultural Sciences.

Authors' contributions

Writing original draft preparation, H.L., M.J.U.; methodology, H.L.; Y.Q.; and S.L.; writing, review, and editing, W.R.; H.L.; M.K.P.; and R.K.V.; resources, C.X.P supervision, C.X.P.; Y.H.; and L.Q.; All authors have read and agreed to the published version of the manuscript.

Funding

This work was supported by,
(1) The National Natural Science Foundation of China (32,301,869, 32,172,051 and 32,401,893),
(2) The National Key R&D Program of China (2023YFD1202800),
(3) The Open Competition Program of Top Ten Critical Priorities of Agricultural Science and Technology Innovation for the 14th Five-Year Plan in Guangdong Province (2022SDZG05),
(4) Guangdong Provincial Key Research and Development Program-Modern Seed Industry (2022B0202060004),
(5) China Agriculture Research System of MOF and MARA (CARS-13),
(6) Guangdong Science and Technology Plan Project (2023B1212060038 and 2024B1212060003),
(7) Guangdong Basic and Applied Basic Research Foundation (2023A1515010098 and 2024A1515010511),
(8) Technology Special Fund of Guangdong Province Agriculture and Rural Affairs Department (2019KJ136-02),
(9) Special Funds for the Revitalization of Agriculture through Seed Industry under the Provincial Rural Revitalization Strategy (2022-NPY-00–022),
(10) Guangzhou Basic and Applied Basic Research Foundation (202,201,010,281, 2023A04J0776 and 2024A04J3870),
(11) Agricultural Competitive Industry Discipline Team Building Project of Guangdong Academy of Agricultural Sciences (202104TD),
(12) Special Fund for Scientific Innovation Strategy-Construction of High-Level Academy of Agriculture Science (R2020PY-JX004, R2020PY-JG005, R2021PY-QY003, R2022YJ-YB3025 and R2023PY-JG007),

(13) The Foundation of Director of Crop Research Institute of Guangdong Academy of Agriculture Sciences/Open Fund of Guangdong Provincial Key Laboratory of Crop Genetic Improvement (202,101, 202,201 and 202,306), (14) The Special Support Program of Guangdong Province (2021TX06N789), (15) The Project of Collaborative Innovation Center of GDAAS (XTXM202203).

Data availability
The raw RNA-seq sequencing data have been deposited at the National Center for Biotechnology Information (NCBI) under the Bio-Project accession PRJNA1045372. As mentioned in the corresponding original literature, the published transcriptomic datasets for key gene expression analysis can be downloaded from the NCBI Sequence Read Archive under accession number SRP033292.

Declarations

Ethics approval and consent to participate
Not applicable.

Consent for publication
Not applicable.

Competing interests
The authors declare no competing interests.

Received: 6 November 2024 / Accepted: 13 June 2025
Published online: 02 July 2025

References

1. Chen XP, Lu Q, Liu H, Zhang JN, Hong YB, Lan HF, et al. Sequencing of cultivated peanut, Arachis hypogaea, yields insights into genome evolution and oil improvement. Mol Plant. 2019;12(7):920–34.
2. Zhuang WJ, Chen H, Yang M, Wang JP, Pandey MK, Zhang C, et al. The genome of cultivated peanut provides insight into legume karyotypes, polyploid evolution and crop domestication. Nat Genet. 2019;51(5):865–76.
3. Kumar R, Pandey MK, Roychoudhry S, Nayyar H, Kepinski S, Varshney RK. Peg biology: Deciphering the molecular megulations involved during peanut peg development. Front Plant Sci. 2019;10:1289.
4. Moctezuma E. The peanut gynophore: A developmental and physiological perspective. Can J Bot. 2003;81(3):183–90.
5. Liu H, Liang X, Lu Q, Li H, Liu H, Li S, et al. Global transcriptome analysis of subterranean pod and seed in peanut (Arachis hypogaea L.) unravels the complexity of fruit development under dark condition. Sci Rep. 2020;10(1):13050.
6. Feng QL, Stalker HT, Pattee HE, Isleib TG. Arachis hypogaea plant recovery through in vitro culture of peg tips. Peanut Sci. 1995;22(2):129–35.
7. Zhu W, Zhang EH, Li HF, Chen XP, Zhu FH, Hong YB, et al. Comparative proteomics analysis of developing peanut aerial and subterranean pods identifies pod swelling related proteins. J Proteomics. 2013;91:172–87.
8. Chen XP, Yang QL, Li HF, Li HY, Hong YB, Pan LJ, et al. Transcriptome-wide sequencing provides insights into geocarpy in peanut (Arachis hypogaea L.). Plant Biotechnol J. 2016;14(5):1215–24.
9. Jacobs WP. Auxin relationships in an intercalary meristem: Further studies on the gynophore of Arachis hypogaea. Am J Bot. 1951;38(4):307–10.
10. Zamski E, Ziv M. Pod formation and its geotropic orientation in the peanut, Arachis hypogaea L., in relation to light and mechanical stimulus. Ann Bot. 1976;40(3):631–6.
11. Ziv M, Kahana O. The role of the peanut (Arachis hypogaea) ovular tissue in the photo-morphogenetic response of the embryo. Plant Sci. 1988;57(2):159–64.
12. Moctezuma E, Feldman LJ. Auxin redistributes upwards in graviresponding gynophores of the peanut plant. Planta. 1999;209(2):180–6.
13. Zhang HY, Wang ML, Liu ZM, Liang QS. Effects of anm cultivate technique on bud differentiation and gynophore elongation of peanut. J Laiyang Agr Univ. 2004;21:203–5.
14. Molinari MDC, Fuganti-Pagliarini R, de Amorim BD, Barbosa EGG, Kafer JM, Marin DR, et al. Comparative aba-responsive transcriptome in soybean cultivars submitted to different levels of drought. Plant Mol Biol Rep. 2023;41(2):260–76.
15. Quamruzzaman M, Ullah MJ, Karim MF, Islam N, Rahman MJ, Sarkar MD. Reproductive development of two groundnut cultivars as influenced by boron and light. Inf Process Agric. 2018;5(2):289–93.
16. Ziv M, Zamski E. Geotropic responses and pod development in gynophore explants of peanut (Arachis hypogaea L.) cultured in vitro. Ann Bot. 1975;39(3):579–83.
17. Shlamovitz N, Ziv M, Zamski E. Light, dark and growth regulator involvement in groundnut (Arachis hypogaea L.) pod development. Plant Growth Regul. 1995;16(1):37–42.
18. Xia H, Zhao CZ, Hou L, Li AQ, Zhao SZ, Bi YP, et al. Transcriptome profiling of peanut gynophores revealed global reprogramming of gene expression during early pod development in darkness. BMC Genomics. 2013;14(1):517.
19. Sun Y, Wang QG, Li Z, Hou L, Dai SJ, Liu W. Comparative proteomics of peanut gynophore development under dark and mechanical stimulation. J Proteome Res. 2013;12(12):5502–11.
20. Cui Y, Su Y, Bian J, Han X, Guo H, Yang Z, et al. Single-nucleus rna and atac sequencing analyses provide molecular insights into early pod development of peanut fruit. Plant Commun. 2024;5(8):100979.
21. Zhao C, Zhao S, Hou L, Xia H, Wang J, Li C, et al. Proteomics analysis reveals differentially activated pathways that operate in peanut gynophores at different developmental stages. BMC Plant Biol. 2015;15:188.
22. Zhu W, Chen XP, Li HF, Zhu FH, Hong YB, Varshney RK, et al. Comparative transcriptome analysis of aerial and subterranean pods development provides insights into seed abortion in peanut. Plant Mol Biol. 2014;85(4–5):395–409.
23. Chen XP, Zhu W, Azam S, Li HY, Zhu FH, Li HF, et al. Deep sequencing analysis of the transcriptomes of peanut aerial and subterranean young pods identifies candidate genes related to early embryo abortion. Plant Biotechnol J. 2013;11(1):115–27.
24. Cui YY, Bian JX, Lv YY, Li JH, Deng XW, Liu XQ. Analysis of the transcriptional dynamics of regulatory genes during peanut pod development caused by darkness and mechanical stress. Front Plant Sci. 2022;13:904162.
25. Molinari MDC, Fuganti-Pagliarini R, Mendonça JA, Barbosa DDA, Marin DR, Mertz-Henning L, et al. Transcriptome analysis using RNA-Seq from experiments with and without biological replicates: A review. Amazonian J Agric Environ Sci. 2021;64:13.
26. Bolger AM, Lohse M, Usadel B. Trimmomatic: A flexible trimmer for illumina sequence data. Bioinformatics. 2014;30(15):2114–20.
27. Kim D, Paggi JM, Park C, Bennett C, Salzberg SL. Graph-based genome alignment and genotyping with hisat2 and hisat-genotype. Nat Biotechnol. 2019;37(8):907–15.
28. Perelo LW, Gabernet G, Straub D, Nahnsen S. How tool combinations in different pipeline versions affect the outcome in rna-seq analysis. NAR Genom Bioinform. 2024;6(1):lqae020.
29. Shumate A, Wong B, Pertea G, Pertea M. Improved transcriptome assembly using a hybrid of long and short reads with stringtie. PLoS Comput Biol. 2022;18(6):e1009730.
30. Pertea G, Pertea M. Gff utilities: Gffread and gffcompare. F1000Res. 2020;9:304.
31. Buchfink B, Xie C, Huson DH. Fast and sensitive protein alignment using diamond. Nat Methods. 2015;12(1):59–60.
32. Zheng Y, Jiao C, Sun HS, Rosli HG, Pombo MA, Zhang PF, et al. Itak: A program for genome-wide prediction and classification of plant transcription factors, transcriptional regulators, and protein kinases. Mol Plant. 2016;9(12):1667–70.
33. Pérez-Rodríguez P, Riaño-Pachón DM, Corrêa LG, Rensing SA, Kersten B, Mueller-Roeber B. Plntfdb: Updated content and new features of the plant transcription factor database. Nucleic Acids Res. 2010;38(Database issue):D822-827.
34. Jin JP, Zhang H, Kong L, Gao G, Luo JC. Planttfdb 3.0: A portal for the functional and evolutionary study of plant transcription factors. Nucleic Acids Res. 2014;42(Database issue):D1182-1187.
35. Liao Y, Smyth GK, Shi W. Featurecounts: An efficient general purpose program for assigning sequence reads to genomic features. Bioinformatics. 2014;30(7):923–30.
36. Love MI, Huber W, Anders S. Moderated estimation of fold change and dispersion for rna-seq data with deseq2. Genome Biol. 2014;15(12):550.
37. Wu T, Hu E, Xu S, Chen M, Guo P, Dai Z, et al. Clusterprofiler 4.0: A universal enrichment tool for interpreting omics data. Innovation (Camb). 2021;2(3):100141.
38. Langfelder P, Horvath S. WGCNA: An R package for weighted correlation network analysis. BMC Bioinformatics. 2008;9:559.
39. Li A, Horvath S. Network module detection: Affinity search technique with the multi-node topological overlap measure. BMC Res Notes. 2009;2:142.

40. Das S, Meher PK, Rai A, Bhar LM, Mandal BN. Statistical approaches for gene selection, hub gene identification and module interaction in gene co-expression network analysis: An application to aluminum stress in soybean (Glycine max l.). PLoS One. 2017;12(1):e0169605.
41. Shannon P, Markiel A, Ozier O, Baliga NS, Wang JT, Ramage D, et al. Cytoscape: A software environment for integrated models of biomolecular interaction networks. Genome Res. 2003;13(11):2498–504.
42. Lv ZH, Zhou DY, Shi XL, Ren JY, Zhang H, Zhong C, et al. Comparative multi-omics analysis reveals lignin accumulation affects peanut pod size. Int J Mol Sci. 2022;23(21):13533.
43. Costa A, Resentini F, Buratti S, Bonza MC. Plant ca(2+)-atpases: From biochemistry to signalling. Biochim Biophys Acta Mol Cell Res. 2023;1870(7):119508.
44. Gao Y, Xu Z, Zhang L, Li S, Wang S, Yang H, et al. Myb61 is regulated by grf4 and promotes nitrogen utilization and biomass production in rice. Nat Commun. 2020;11(1):5219.
45. Guénin S, Hardouin J, Paynel F, Müller K, Mongelard G, Driouich A, et al. Atpme3, a ubiquitous cell wall pectin methylesterase of Arabidopsis thaliana, alters the metabolism of cruciferin seed storage proteins during post-germinative growth of seedlings. J Exp Bot. 2017;68(5):1083–95.
46. Guénin S, Mareck A, Rayon C, Lamour R, AssoumouNdong Y, Domon JM, et al. Identification of pectin methylesterase 3 as a basic pectin methylesterase isoform involved in adventitious rooting in Arabidopsis thaliana. New Phytol. 2011;192(1):114–26.
47. Lan W, Zheng S, Yang P, Qiu YH, Xu Y, Miao Y. Establishment of a landscape of upl5-ubiquitinated on multiple subcellular components of leaf senescence cell in arabidopsis. Int J Mol Sci. 2022;23(10):5754.
48. Zhao XB, Li CJ, Zhang H, Yan CX, Sun QX, Wang J, et al. Alternative splicing profiling provides insights into the molecular mechanisms of peanut peg development. BMC Plant Biol. 2020;20(1):488.
49. Fenn MA, Giovannoni JJ. Phytohormones in fruit development and maturation. Plant J. 2021;105(2):446–58.
50. Molinari MDC, Fuganti-Pagliarini R, Marcolino-Gomes J, de Amorim BD, Rockenbach Marin SR, Mertz-Henning LM, et al. Flower and pod genes involved in soybean sensitivity to drought. J Plant Interact. 2021;16(1):187–200.
51. Molinari MDC, Fuganti-Pagliarini R, Barbosa DA, Marin SRR, Marin DR, Rech EL, et al. Flowering process in soybean under water deficit conditions: a review on genetic aspects. Genet Mol Biol. 2021;45(1):e20210016.
52. Shaharoona B, Arshad M, Khalid A. Differential response of etiolated pea seedlings to inoculation with rhizobacteria capable of utilizing 1-aminocydopropane-1-carboxylate or l-methionine. J Microbiol. 2007;45(1):15–20.
53. Shushu DD, Cutter EG. Growth of the gynophore of the peanut Arachis hypogaea. 2. Regulation of growth. Can J Bot. 1990;68(5):965–78.
54. Tian H, Lv B, Ding T, Bai M, Ding Z. Auxin-br interaction regulates plant growth and development. Front Plant Sci. 2017;8:2256.
55. Dave A, Hernández ML, He Z, Andriotis VM, Vaistij FE, Larson TR, et al. 12-oxo-phytodienoic acid accumulation during seed development represses seed germination in arabidopsis. Plant Cell. 2011;23(2):583–99.
56. Majhi BB, Sessa G. Overexpression of BSK5 in Arabidopsis thaliana provides enhanced disease resistance. Plant Signal Behav. 2019;14(9):e1637665.
57. Pfeiffer A, Shi H, Tepperman JM, Zhang Y, Quail PH. Combinatorial complexity in a transcriptionally centered signaling hub in arabidopsis. Mol Plant. 2014;7(11):1598–618.
58. Hayes S, Pantazopoulou CK, van Gelderen K, Reinen E, Tween AL, Sharma A, et al. Soil salinity limits plant shade avoidance. Curr Biol. 2019;29(10):1669-1676.e1664.
59. Liu QQ, Luo L, Zheng LQ. Lignins: Biosynthesis and biological functions in plants. Int J Mol Sci. 2018;19(2):335.
60. Schuetz M, Benske A, Smith RA, Watanabe Y, Tobimatsu Y, Ralph J, et al. Laccases direct lignification in the discrete secondary cell wall domains of protoxylem. Plant Physiol. 2014;166(2):798–807.
61. Li X, Bonawitz ND, Weng JK, Chapple C. The growth reduction associated with repressed lignin biosynthesis in Arabidopsis thaliana is independent of flavonoids. Plant Cell. 2010;22(5):1620–32.
62. Parrotta L, Guerriero G, Sergeant K, Cai G, Hausman JF. Target or barrier? The cell wall of early- and later-diverging plants vs cadmium toxicity: Differences in the response mechanisms. Front Plant Sci. 2015;6:133.
63. Jia X-m, Zhu Y-f, Hu Y, Zhang R, Cheng L, Zhu Z-l, et al. Integrated physiologic, proteomic, and metabolomic analyses of Malus halliana adaptation to saline–alkali stress. Hortic Res. 2019;6:91.
64. Yang S, Wang J, Tang Z, Guo F, Zhang Y, Zhang J, et al. Transcriptome of peanut kernel and shell reveals the mechanism of calcium on peanut pod development. Sci Rep. 2020;10(1):15723.
65. Zharare G, Blamey F, Asher C. Initiation and morphogenesis of groundnut (Arachis hypogaea L.) pods in solution culture. Ann Botany. 1998;81(3):391–6.
66. White PJ, Broadley MR. Calcium in plants. Ann Bot. 2003;92(4):487–511.

Publisher's Note